

On the identification of SFRC tensile constitutive behaviour

Marco di Prisco, Roberto Felicetti & Francesco Iorio

Department of Structural Engineering, Politecnico di Milano, Italy

Ravindra Gettu

Universitat Politècnica de Catalunya, Barcelona, Spain

ABSTRACT: A σ - ϵ approach proposed by RILEM Technical Commission to design steel fibre reinforced concrete (SFRC) structures is herein discussed. The method is based on the identification of equivalent tensile strengths related to the energy dissipated up to certain kinematic thresholds in a third point bending test with an assigned geometry. This approach extends usual R/C computations based on plane-section assumption without an explicit definition of a structural or material characteristic length, though a softening constitutive law was introduced. On the basis of two experimental programmes investigating beams with different depth, a check of this approach is attempted. Only hooked steel fibres were considered with 80 kg/m^3 maximum fibre amount, since this limit can be regarded as an economical upper bound for the majority of concrete structures. The results confirm a quite satisfactory prediction for beam up to 150 mm deep, but sometimes a dangerous overestimation of the maximum load is observed for deeper structures. A comparison with a F.E. smeared-crack approach highlights the limits of the simplified approach proposed for design.

1 INTRODUCTION

Steel fibre reinforced concrete is a material that shows localisation and softening in uniaxial tension even with large amount of fibres (up to 3%). Nevertheless, the bending behaviour can exhibit ductility and small scatter, if the failure of fibres is prevented. This goal can be attained adapting the concrete matrix to fibre characteristics.

Kooiman (2000) has recently presented good predictions based only on the knowledge of compressive strength and fibre length. However, according to RILEM recommendations (2000a,b), the modelling of bending response can be carried out by identifying the tensile constitutive behaviour by means of uniaxial tension or bending tests.

Both the approaches are herein exploited in order to understand the related limitations and judge on reliability and applicability in design. The main doubt is connected with the σ - ϵ relationship proposed by RILEM (2000b), where the strain of the break-point is fixed with respect to the peak (Fig.7).

The most significant branch in the tensile constitutive relationship usually starts from the break-point and corresponds to fibre pull-out. However, especially when the structure is unnotched, the peak load could depend on the matrix fracture energy G_f , which is neglected in this approach. The investigation reveals as no size effect is taken into account according to RILEM approach,

and this is acceptable only if hardening behaviour caused by fibre pull-out prevails in bending.

2 EXPERIMENTAL RESULTS

Two experimental programmes are herein presented, aimed to predict the behaviour of FRC structures with different depth (40±400 mm). The tests were performed in the Laboratories of Milan and Barcelona Universities of Technology (di Prisco & Felicetti 1999; Moguel 1999). Only hooked steel fibres were considered, with 80 kg/m^3 maximum fibre amount. Two different concrete mixes were adopted, as specified in Table 1. The cubic compressive strength of mix 1 was 110 MPa (age: 21±28 days), whereas the cylindrical compressive strength of mix 2 was 75 MPa (age: 60 days).

Mix 1 was adopted also to make precast thin-webbed roof structures with an open cross-section (di Prisco et al., 2000). Therefore, zinc-coated steel fibres were preferred. The tensile behaviour of this concrete was first identified according to RILEM recommendations (2000b). Furthermore, the special application of this mix suggested to check the bending behaviour through proper unnotched specimens prepared by sawing a thin plate. A special care was devoted to the direction of tensile stress in relation to the cast direction, because the small thickness of the specimens and the vibration after casting could significantly affect the fibre-

Table 1 – Concrete mix-designs.

Components	Content by weight [kg/m ³]	
	Mix 1	Mix 2
cement I 52.5 R	405	457
microsilica	45	46
Sand 0-5 mm	-	869
sieved sand 0-3 mm	110	-
natural sand 0-12 mm	960	-
gravel 5-12 mm	-	869
gravel 8-15 mm	810	-
acrylic superplasticizers	12	17.8
water	125	143
High-carbon steel fibre 30/0.5	-	80
Low-carbon steel fibre 30/0.6	50	-

orientation factor (di Prisco & Felicetti, 1999). Previous experiences showed that a change in the cast direction could markedly affect the total fracture energy of the SFR concrete (up to 300% and even more; di Prisco and Felicetti, 1998).

Two depth sizes ($h = 40$ and 60 mm) were investigated. A closed-loop electro-mechanical press (INSTRON 8562) was adopted. The results of the third-point bending tests are shown in terms of equivalent stress (σ_{eq}) versus crack opening displacement (COD - Fig. 2). The deformation was measured along three gauge lengths (80-70-80 mm) by arranging five LVDTs on the bottom side of the beam. The displacement pertaining to the gauge length where the main crack occurred was regarded as the COD. The equivalent stress was computed by dividing the bending moment applied by the elastic flexural modulus $W_e = bh^2/6$. Each test was repeated on two nominally identical specimens: the scatter is quite large (about 25%), but no significant influence of the specimen depth arose.

In the same figure, the results of the central point bending tests carried out according to RILEM recommendations (2000) are also presented. In this case the specimens were notched (depth $h = 150$ mm - notch depth $a = 25$ mm) and the crack opening is a crack mouth opening displacement (gauge length = 50 mm). The ligament length ($h - a$) has been taken into account to work out the equivalent stress.

The notch reduces the stress at cracking (-15%), whereas the increased depth allows a longer crack propagation, with a relatively lower matrix contribution to the peak-load (-10%) and a smoother transition to the fibre pull-out stage. RILEM tests show an abrupt decrease of the load when the COD exceeds 0.6-0.7 mm. This trend causes a significant reduction of work of fracture (i.e. residual strength).

Finally, uniaxial tensile tests on notched prismatic specimens were carried out (the geometry

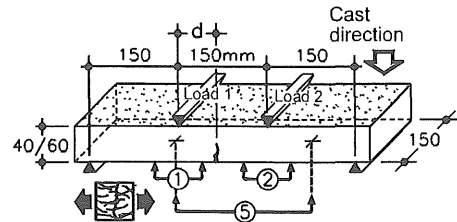


Fig.1 – Third point bending test set-up.

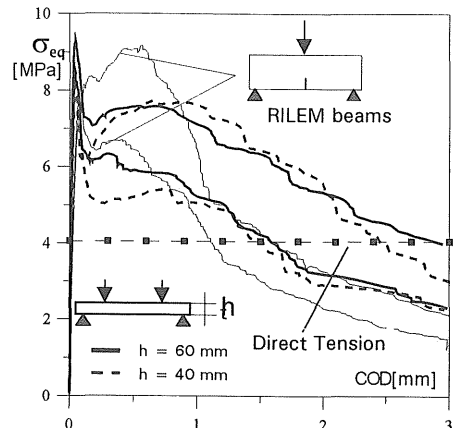


Fig.2 – Equivalent stress-COD curves in bending and equivalent strength in direct tension (mix 1 concrete).

and the test set-up are shown in Fig.3a). Both the effect of specimen size (size ratio 1:3) and boundary conditions (rotating and fixed end-platen) were investigated. In the latter case, the rotation of the press bearing plates was prevented by means of four adjustable steel bars (Fig.3b).

The results are expressed in terms of average stress (P/A_0) versus average crack opening displacement (Fig.4). With reference to the peak stress, a pronounced size effect was observed. By contrast, the residual strength showed higher values for the largest specimen.

It's worth to note that the average tensile strength identified by uniaxial tension test is always smaller than that identified by bending test (-6% at average COD=0.3mm and -18% at average COD=1.5mm). This result is emphasised by superposing to the bending test curves the equivalent bending strength identified by direct tension tests (Fig.2). This value was computed on the basis of the average tensile strength up to a COD of 1.5 mm. A multiplying factor three takes into account the relation between the elastic and the rigid-plastic flexural moduli (with the assumption of a tensile stress-block pertaining to the whole cross section in the latter case).

With reference to the rotational stiffness of the loading platens, a weak reduction of the peak stress and a scatter increase were observed.

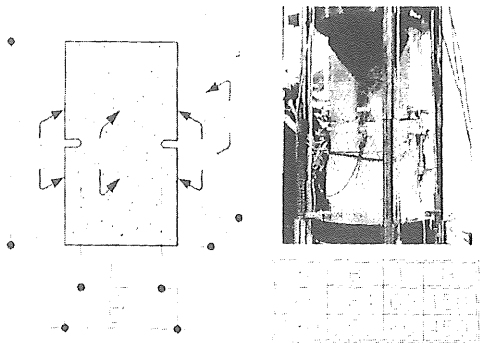


Fig.3 – Uniaxial tension: specimen geometry and test set-up.

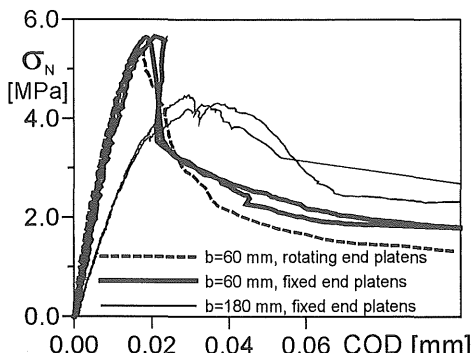


Fig. 4 - Average stress-COD curves in uniaxial tension.

In the second experimental programme, 150 mm deep notched beams were tested as well (Mix 2 - Moguel, 1999). A hardening behaviour in bending was observed, as it is shown in Fig.6. Though the notch ratio of these specimens does not coincide with that suggested by RILEM, the difference was considered negligible in the material characterisation. The equivalent tensile strengths computed according to RILEM recommendations (2000b) highlights the residual strength increase supplied by high carbon steel fibres (Table 2).

Two 320 mm deep beams characterised by a higher notch ratio were also tested ($a/h = 0.275$; Figs.5, 6). Their investigation is instrumental in assessing size effect when the collapse is governed by fibre pull-out. Finally, two 400 mm deep unnotched beams ($b = 100$ mm - $L = 1400$ mm) were tested adopting a central point loading set-up. These results are discussed in the following.

Table 2 – Mechanical parameters identified according to RILEM recommendations.

	f_{ct} [MPa]	$f_{eq,2}$ [MPa]	$f_{eq,3}$ [MPa]
Mix 1	5.6	7.5	4.28
Mix 2	5.7	12.9	11.2

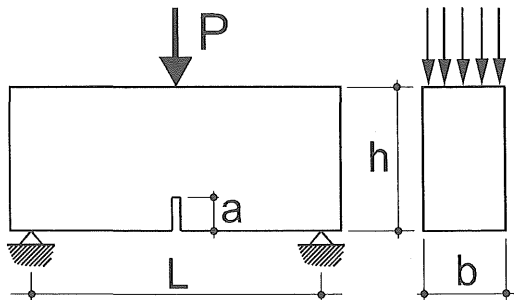


Fig. 5 – Large specimens geometry and test set-up.

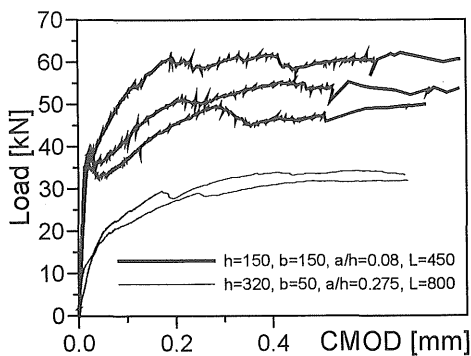


Fig.6 – Large specimens load-CMOD curves (mix 2 concrete).

3 σ - ϵ APPROACH

The main assumption in the σ - ϵ approach suggested by RILEM recommendations (2000b) is the kinematic constraint of the plane-section. The idea is to create an abrupt discontinuity in the curvature description along the beam axis to model the elasto-softened region. This means that no localisation is modelled and a unique curvature for both the compressed and the cracked zone in the critical piece of beam is adopted.

The kinematic description of the member is completed by assuming a structural characteristic length L_{cs} , which governs the size of the critical piece of the beam and grows with the crack propagation. The crack length (ξ in Fig.7) can be computed knowing the position where the tensile peak strength f_{ct} is reached. This approach needs a stress-strain constitutive law that is described as a function of the dissipated energy in a three point bending test. It is worth to note that no size-effect can be modelled following this approach, because the bending moment always depends on the square of the depth.

This approach has been applied to model a thin plate in a third point loading scheme (mix 1; $h = 60$ mm): the bending response and the width evolution of the cracked portion are shown in Fig.8.

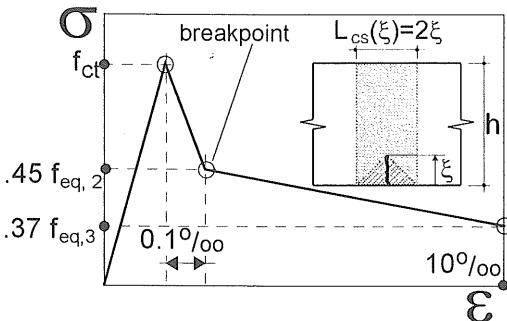


Fig.7 – RILEM model: main assumptions and reference values in the σ - ϵ constitutive relationship.

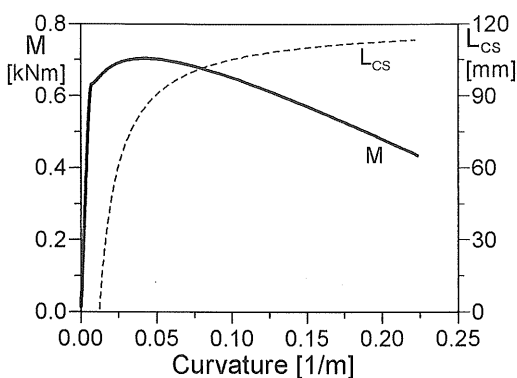


Fig.8 – Mechanical response for a thin slab ($t=60$ mm) in bending and size evolution of the beam portion subjected to crack localisation.

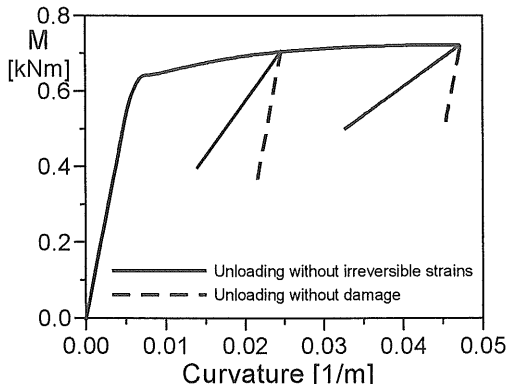


Fig. 9 – Constitutive relationship in bending: effect of the limit assumptions for the unloading path.

In the hardening branch the unloading response has been also investigated, assuming that the inelastic strain is either totally irreversible (no damage) or reversible (Fig.9). The two hypotheses have been checked in terms of loading point de-

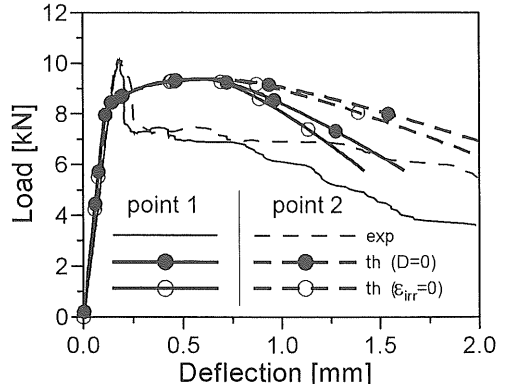


Fig.10 – Thin plate behaviour in bending: influence of the unloading path on the loading points deflection.

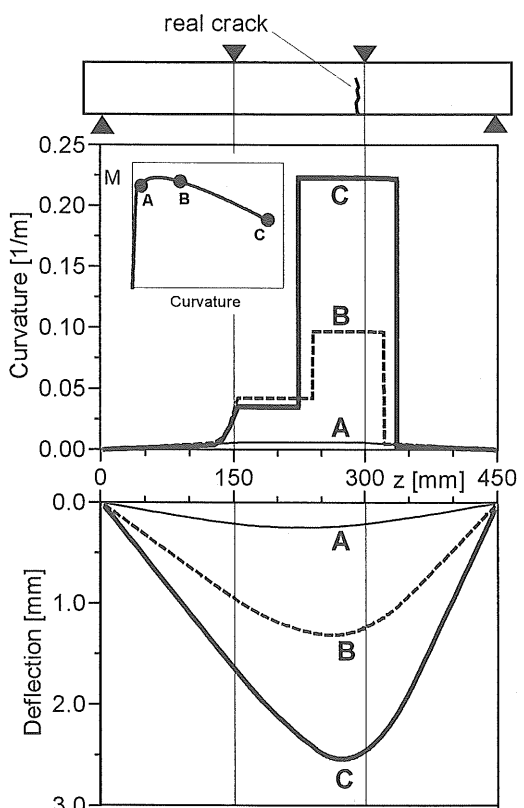


Fig.11 – Curvature profile and deformed shape derived with the beam-section approach.

flection, and a more realistic post-peak slope can be observed when damage is neglected. The curvature profile along the beam axis shows that the inelastic deformation in the cracked zone remains spread during softening (Fig.11).

4 F.E. APPROACH

Besides the σ - ϵ approach, aimed to be used in a plane section model, RILEM TC-TDF 162 is providing two further documents suggesting a σ - w approach addressed to F.E. modelling. In the latter approach, the mechanical parameters are identified by means of the uniaxial tensile test. Following the σ - w approach, a smeared crack analysis is carried out by means of a non-local damage model (di Prisco & Mazars, 1996).

The fixed-end platens uniaxial tension test was reproduced by adopting a parabolic pre-peak law and a three-linear softening law (Fig.12b, c). The softening branch starts from the tensile strength at peak with the same slope as plain concrete and reaches a constant residual strength corresponding to fibre pull-out mechanism.

The material characteristic length was regarded as a constant and set equal to the maximum aggregate size as in plain concrete (di Prisco et al., 1999; Ferrara & di Prisco, 2001). The same model was then adopted to reproduce a rotating end-platens test with the same geometry. A small defect on one notch tip (tensile strength reduced by 10%) allowed to activate an asymmetric crack propagation.

The results are compared in terms of COD on the notched sides of the specimen. The rotation and the crack opening of the model fit pretty well the experimental curves (Figs.12d-f).

Finally, to judge on the limitations introduced by the σ - ϵ approach, a simple thin plate bending case was investigated (Fig.13). The F.E. and the plane section models are compared in terms of bending response (Fig.14). The latter model was applied using both the σ - ϵ relationship identified through the RILEM procedure (P.S.1 - see Fig. 7) and the σ - w law adopted in F.E. and derived from the uniaxial tension test (P.S.2 - constitutive law of Fig.12b after multiplying ϵ by the material characteristic length).

In order to implement the σ - w law in the plane section (σ - ϵ) approach, the crack opening w needs to be smeared along an average structural length. In the simulation, the average size of the elasto-softened beam piece (i.e. the beam depth) was adopted. Despite the simplicity of this model, the improvement is well recognisable. However, the plane-section kinematic constraint still stabilises the crack propagation with respect to the F.E. model.

The strain profiles along the beam depth at the peak and at the last computational step (average COD = 1.5 mm) highlight that plane-section are restored at a distance from the crack plane comparable to the beam depth. At the peak, the almost bilinear strain profile close to the crack plane is fully disregarded by the σ - ϵ approach, that smears the localised strain in a softened region characterised by a unique curvature value.

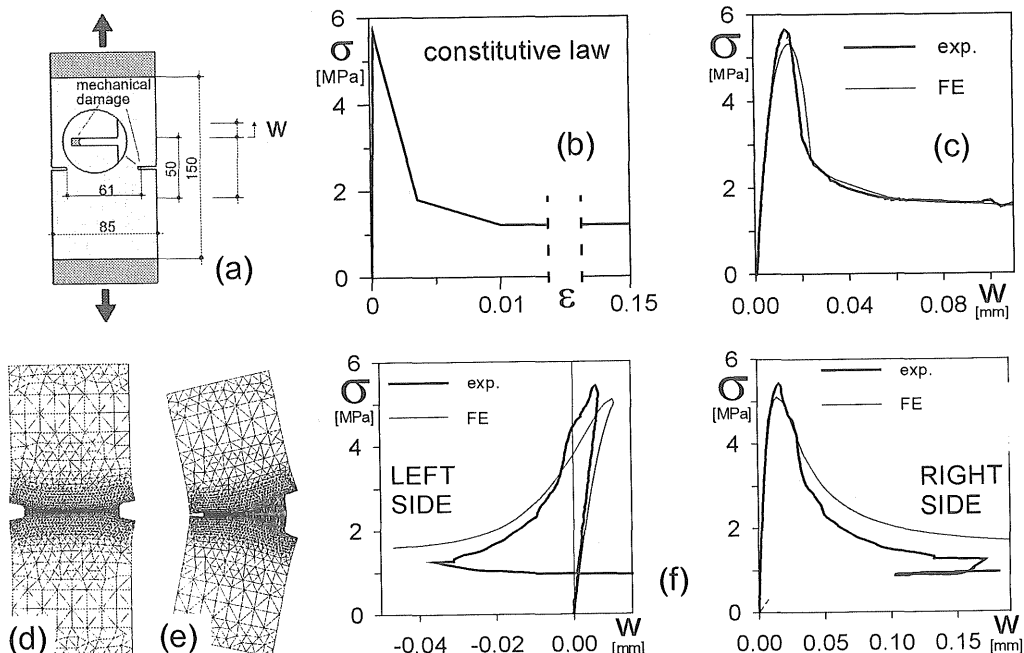


Fig.12 – Uniaxial tension tests modelling: (a) fixed platen set-up; (b) constitutive law adopted; (c) fixed end-platens test reproduction; (d, e) rotating end-platens F.E. model deformed shapes; (f) experimental and numerical average stress-COD curves.

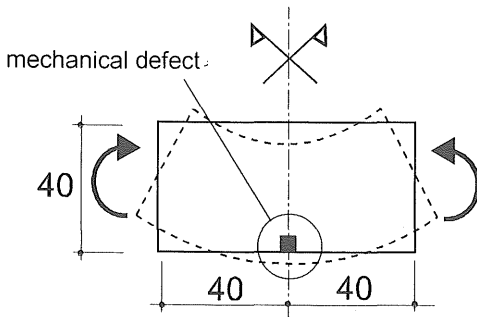


Fig.13 – Thin plate bending test investigated via F.E. and plane-section approaches.

5 TEST MODELLING

Following the plane section approach, the three point bending tests adopted to identify the RILEM constitutive tensile laws were first modelled (Fig.16). The material identification procedure (based on uniaxial tension or bending tests) affects both the residual bending moment and the global response, passing from a brittle to a ductile behaviour (Fig.16a). Given the same constitutive relationship, the kinematic model (Finite Element or Plane Section) exerts a weak influence. As expected, it affects only the first part of the curve, connected to the fracture of the concrete matrix.

In the fibre pull-out stage, the plane section model seems to overestimate the deflection, owing to the law that controls the structural length growth.

About the thin plate modelling (Fig.17), the tests are quite well reproduced by the σ - ϵ approach, in consideration of the simplicity of the model. The prediction cannot fit the experimental peak and consequently the brittleness detected in the post-peak region. Nevertheless, the introduction of suitable safety factors, as suggested by RILEM recommendations, could assure a satisfactory reliability with reference to the ultimate limit states.

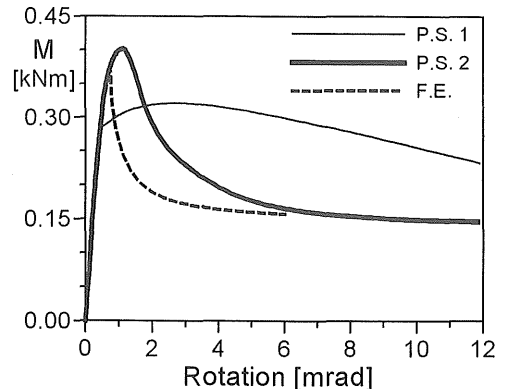
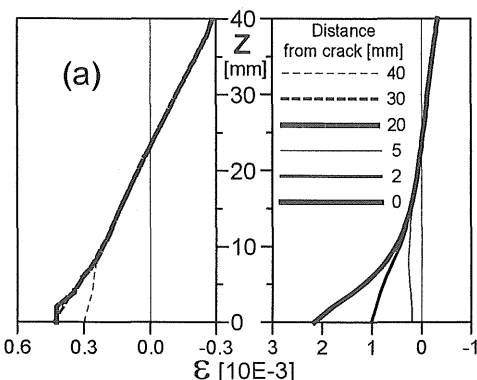


Fig.14 – Modelling of bending behaviour: influence of the kinematic model and of the tensile constitutive relationship.

The small depth of the plates, which could increase the orientation factor and consequently the equivalent tensile strengths (di Prisco, 2000), does not exert a significant effect in the bending response with reference to the plane-section modelling.

Finally, the bending response of deeper beams was investigated (Moguel, 1999). The plane-section modelling fits well the notched beams and largely overestimates the unnotched ones. However, the drastic drop shown by the latter tests was not expected. The hardening shown after cracking by identification tests could not justify such an important effect in the fibre pull-out stage.

In the plane-section model, a weak size effect could be introduced if the constitutive relationship is based on the σ - w tensile curve. As a matter of fact, the structural length that is needed to smear the crack opening in the elasto-softened region is usually regarded as a function of the beam depth ($L_{cs}=h/2$ as suggested by Kooiman, 2000 – Fig.20).

Nevertheless, all of the experimental tests did not exhibit nominal tensile strength variations with the beam depth, with the only exception of the mix 2 unnotched beams (Fig.20).

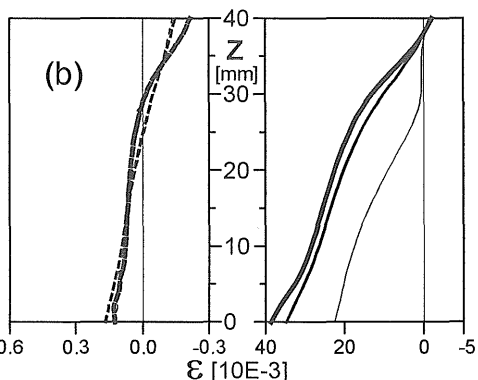


Fig.15 – F.E. thin plate model: strain profiles at different distances from the crack plane: (a) at the peak; (b) at the last step.

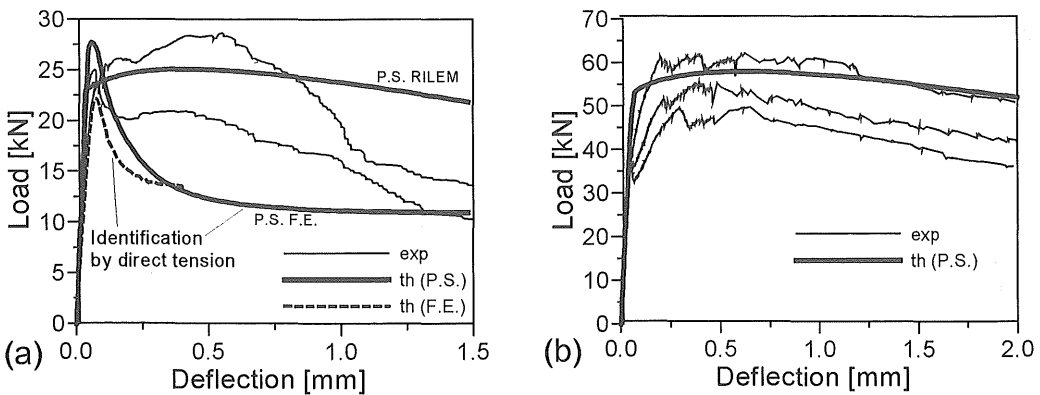


Fig.16 – Modelling of three point bending tests used for identification: (a) mix 1; (b) mix 2.

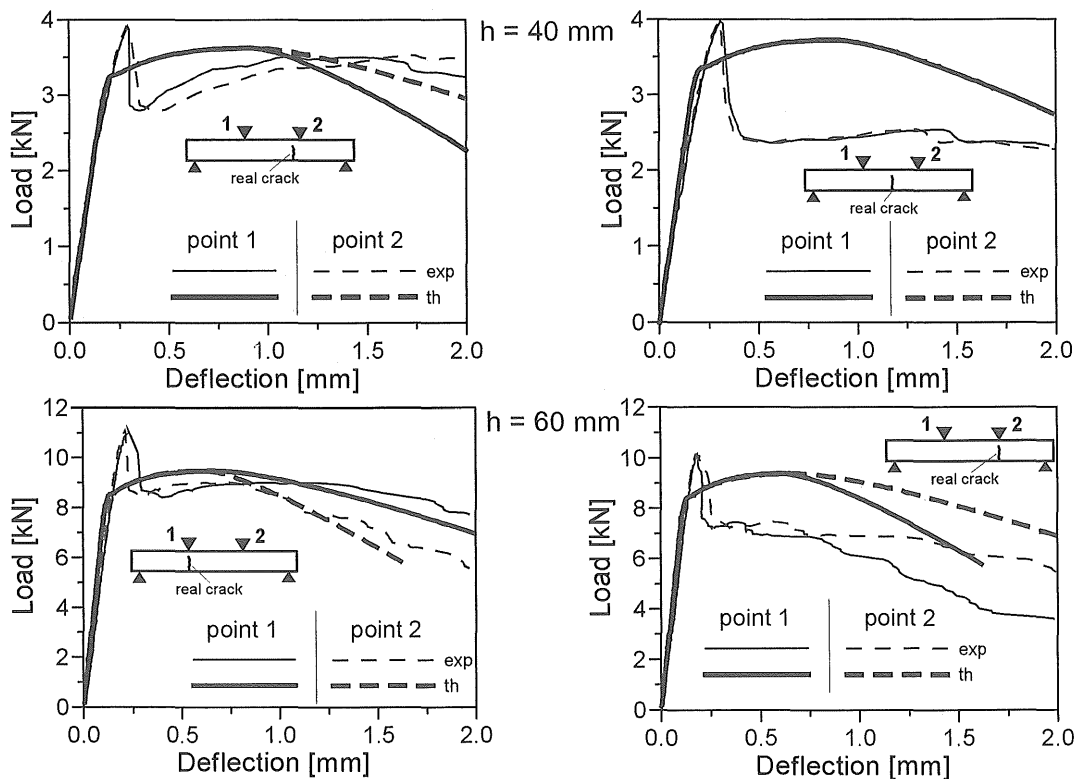


Fig. 17 – Thin plate modelling ($h = 40-60$ mm) according to RILEM recommendations and based on a known crack location.

6 CONCLUDING REMARKS

The $\sigma\text{-}\epsilon$ approach proposed by RILEM recommendations can be used in design to model the bending response of a structure. Provided that a very brittle softening behaviour due to the fibre failure does not occur, this method gives satisfactory results, although it risks to overestimate the ductility in bending when fibre pull-out prevails. A more careful

identification of the tensile constitutive law can improve the test fitting. Even if the method cannot reproduce size-effect, this phenomenon is strongly reduced by steel fibres and concerns essentially with the crack formation in the matrix.

By contrast a $\sigma\text{-}w$ approach based on uniaxial tension tests gives a safer characterisation of the tensile behaviour, even if it requires a larger computational effort and thus it cannot be proposed

for common design. In a smeared approach, a constant material characteristic length allows a refined reproduction of the structural tensile response, provided that a good calibration of the softening constitutive law is fulfilled.

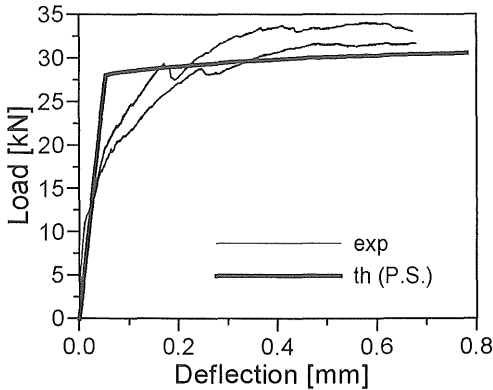


Fig.18 – Deep cross section modelling via the RILEM approach: notched beams ($h=320\text{mm}$ - $a/h=0.275$ - $L=800\text{mm}$).

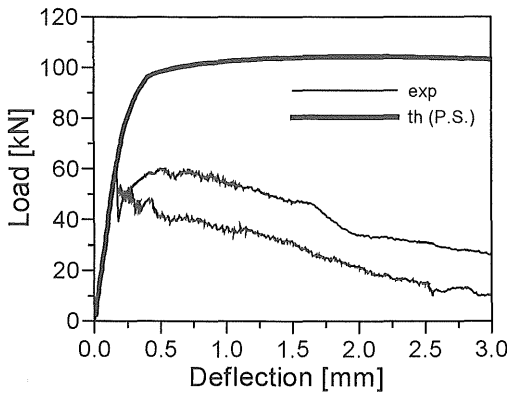


Fig.19 – Deep cross section modelling via the RILEM approach: unnotched beams ($h=400\text{mm}$ - $L=1400\text{ mm}$).

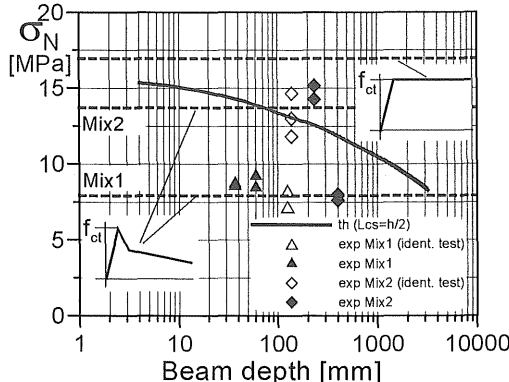


Fig.20 – Size effect with the assumption of plane-section model and half beam depth as the structural length L_{cs} .

ACKNOWLEDGEMENTS

The research has been financed by MURST (Integrated Action Italy-Spain).

REFERENCES

- di Prisco, M. & Mazars, J. 1996. Crush-Crack: a Non-local Damage Model for Concrete, *Mechanics of Cohesive-Frictional Materials and Structures*, 1: 321-347.
- di Prisco, M. & Felicetti R. 1998. On Fatigue of Plain and Fiber Reinforced-Concrete Ground-Slabs, *Technical Report n.1a/98*, Research Project No.1567-1994, Dep. of Struct. Engrg..
- di Prisco, M., Felicetti, R., Gambarova, P. 1999. On the evaluation of the characteristic length in high strength concrete. In A. Azizinamini, D. Darwin and C. French (eds), *High Strength Concrete*: 377-390. Reston, Virginia, ASCE.
- di Prisco, M. & Felicetti, R. 1999. HSC Thin-Web Roof-Elements: an Experimental Investigation on Steel fibre Benefits. *Proc. 5th Int. Symp. on Utilization of HS/HP Concrete*: 546-555. Sandefjord, Norway.
- di Prisco M., Felicetti R. and Iorio, F. 2000. FRHPC precast roof elements: from constitutive to structural behaviour in bending. *Proc. of the, Fifth RILEM Symp. on Fibre Reinforced Concrete BEFIB*: 233-243, Lyon, France. Cachan, France RILEM.
- di Prisco, M. 2000. Design of SFRC precast roof elements. In M. di Prisco & G. Toniolo (eds), *Structural Applications of steel fibre reinforced concrete*: 33-47. Milan, CTE Press.
- Ferrara, L. & di Prisco, M. (in press). Mode I fracture behavior in concrete: non-local damage modelling, *Journal of Engineering Mechanics –ASCE*.
- Ferrara, L. & Gettu, R. 2000. Non-local damage analysis of three-point bending tests on SFRC notched beams, *Proc. of the Fifth RILEM Symp. on Fibre Reinforced Concretes BEFIB*: 357-367, Lyon, France. Cachan, France RILEM.
- Kooiman A.G. 2000. Modelling steel fibre reinforced concrete for structural design. Ph.D. Thesis Technical University Delft. Optima Grafische Communicatie, Rotterdam.
- Moguel, H.S. 1999. Flexural toughness characterisation of steel fibre reinforced concrete – study of experimental methodologies and size effects. Ph.D. Thesis Universitat Politècnica de Catalunya, Barcelona.
- RILEM TC162-TDF. 2000a. Test and Design Methods for Steel Fibre Reinforced Concrete: Recommendations. Bending test. *Materials and Structures*, 33 (225): 3-5.
- RILEM TC162-TDF. 2000b. Test and Design Methods for Steel Fibre Reinforced Concrete: Recommendations. σ - ϵ -Design method. *Materials and Structures*, 33 (226): 75-81.